Nuclear Matter with Quark-Meson Coupling I: Comparison of Nontopological Soliton Models

Nir Barnea*and Timothy S. Walhout†

ECT, European Centre for Theoretical Studies in Nuclear Physics and Related Areas, Strada delle Tabarelle 286, I-38050 Villazzano (Trento), Italy*

and

Istituto Nazionale di Fisica Nucleare, Gruppo collegato di Trento

February 9, 2008

Abstract

A system of nontopological solitons interacting through scalar and vector meson exchange is used to model dense nuclear matter. The models studied are of the Friedberg-Lee type, which exhibit dynamical bag formation due to the coupling of quarks to a scalar composite gluon field σ. It is shown that the high density behavior of such models in the Wigner-Seitz approximation depends essentially on the leading power of the quark-σ coupling vertex. By insisting that the parameters of any soliton model be chosen to reproduce single nucleon properties, this high-density behavior then selects a promising class of models that better fit the empirical results — the chiral chromodielectric models. It is shown that one can adjust the model to obtain saturation as well as an increase of the proton charge radius with nuclear density. These two phenomena depend on the presence of a scalar meson and were not found in other nuclear matter calculations based on Friedberg-Lee type models.

PACS: 24.85.+p, 12.39.Ki, 21.65.+f

Keywords: Nontopological Soliton, Chiral Chromodielectric Model, Friedberg-Lee Model, Nuclear Matter

*e-mail: barnea@ect.it

†e-mail: walhout@ect.it

1 Introduction

Ever since the advent of quantum chromodynamics (QCD) it has been popular to describe the nucleon in terms of bag or soliton models. There are many versions of such models, characterized by two extremes: the MIT bag model [1], where the nucleon consists of just constituent quarks arbitrarily restricted in a given volume, and the Skyrme model [2], where there are no quarks and the nucleon is instead a topological soliton of the pion field. Other models interpolate between these two extremes, seeking to combine the obvious emphases on the structure of nucleons within the MIT bag model and on nuclear interactions via meson exchange within the Skyrme model. For example, chiral bag models [3] surround an MIT-like bag of quarks with a Skyrme-like cloud of pions (and perhaps other mesons as well). Clearly, each such model attempts to balance between low-energy degrees of freedom — the mesons — and high-energy degrees of freedom — the quarks (and possibly gluons as well). Our aim here is to develop a model that as simply as possible, but without losing essential physics, combines quark and meson degrees of freedom. This task is made more difficult by the "Cheshire cat principle" [4], an extrapolation of results found from chiral bag models, which find that low-energy nucleon properties are largely insensitive to the size of the quark bag. As the bag shrinks, the meson cloud forms more and more of the nuclear structure. To select a model, we must study nuclear properties that distinguish between a bag of quarks and a cloud of mesons.

An obvious testing ground for any bag or soliton model is dense baryon matter, where the structure of individual nucleons will become as important as the interactions between neighboring nucleons. Preferably, the model will have a dynamical formation of the bag or soliton, for then one can treat the transition to a quark-gluon plasma consistently. Surprisingly enough, the Skyrme model, which may be thought of as a chiral bag model with the quark bag shrunk to zero size, does predict a dynamical transition to a phase of solitons of fractional baryon number at high densities [5]; however, identifying this phase with a quark-gluon plasma is certainly problematic. Thus in this paper we study dense nuclear matter in a set of models known as non-topological soliton (NTS) models. In particular, we study the Friedberg-Lee (FL) model [6] and a class of related models, the chiral chromodielectric (χCD) models [7, 8], as well as extensions of these models (or, one might argue, approximations to these models) that explicitly include couplings to mesons. These models, based upon general arguments from QCD, are characterized by the coupling of quarks to a scalar field σ that has a nonzero vacuum expectation field. This field is understood to be a composite gluon field. The interaction between the quarks and scalar field leads to a dynamical confinement mechanism, with the quarks carving a hole in the background scalar field. The structure of this bag depends precisely on how the quarks couple to the scalar field, and it is this coupling that distinguishes the various models we study here. All these models reproduce single nucleon properties reasonably well — indeed, chiral bag models show that single nucleon properties are relatively insensitive to the structure of the quark bag. We must look at high densities, where the bags begin to overlap, to see the differences between models with different quark-σ couplings.

In the last few years there also has been considerable interest in the application of the quark-meson coupling (QMC) model to study the nuclear matter equation of state, as well as medium effects on the nucleon structure and nucleon-meson coupling, motivated by the apparent success of the Walecka QHD models [9, 10] in describing the properties of nuclear matter. The QMC model, initially suggested by Guichon [11], consists of non-overlapping nucleon (MIT) bags that interact through the exchange of scalar and vector mesons in the mean-field approximation (MFA). This model has been generalized to include Fermi motion and center of mass corrections [12] and was applied to nuclear matter (see [13] and references therein) and also to finite nuclei [14, 15]. Of course, the assumption that the nucleons can be regarded as non-overlapping bags is only valid at low density, where these models seem to capture the essential physics. Already at nuclear saturation density, however, the internucleon separation is comparable to the nucleon radius, and at higher densities the assumption that the bags do not overlap clearly breaks down. This assumption becomes even more questionable when a modification of the bag constant in nuclear matter is taken into account. Jin and Jennings [16] and Müller and Jennings [13] have recently shown that the introduction of a density-dependent bag constant can reproduce the EMC effect and reconcile the QMC results with those of the Walecka QHD-I model [9]. As a result [13] the bag radius grows with increasing density and the overlapping of the bags starts just above nuclear saturation density.

To take into account the effects from overlapping nucleon bags — that is, to study a nuclear liquid rather a nuclear gas — it is clearly of interest to introduce some dynamics in the confining mechanism. Thus we are led to replace the MIT bag model by a NTS model. Although the study of nuclear matter properties was begun long ago (see [8] and references therein) and was carried out with different soliton models and with different levels of sophistication (see [17, 18] and references therein), none of these calculations included the effect of background meson fields on nuclear matter. Now, in principle, the non-topological soliton models — in particular, the χCD model, which in its full form includes perturbative gluon exchange — contain sea quarks and meson exchange explicitly. However, in practice it is very difficult to deal with anything besides the nuclear constituent quarks. In the interest of simplicity (and at the sacrifice of consistency), we extend our NTS models to include explicitly meson degrees of freedom. (Such an extension has been referred to as the local uniform approximation to χCD in [19].)

In the following, then, we shall study a system of non-topological solitons interacting via the exchange of scalar and vector mesons within the MFA. In modeling nuclear matter each soliton is centered in a spherical Wigner-Seitz (WS) cell. It has been argued that the choice of a spherical WS cell is more appropriate for a fluid phase than a crystal as it represents an angular average over neighbouring sites. We consider two further approximations: in one, the WS calculation is simply used to provide an effective nucleon mass and the kinetic energy is then taken to be that of a Fermi gas, thus providing the correct low-density limit. A second approximation uses a Bloch-like boundary condition to calculate the band structure of the quark states. Neither of these approximations is quite satisfactory, and the second paper of this series is devoted to improving the modeling of a liquid of solitons. Nevertheless, we can still hope that the major qualitive features of dense nuclear matter will be reproduced even given the two approximations used here. Indeed, we find some encouraging results such as

nuclear saturation and an increase of the proton rms with nuclear density. These effects are shown to derive from the background meson fields, which have a considerable effect on the formation of energy bands in nuclear matter.

In this paper we limit our attention to Friedberg-Lee soliton type models extended to include the meson fields. The non-topological soliton models are presented in Sec. 2. The Wigner-Seitz approximation is then discussed in Sec. 3. In Sec. 4 we study in some detail the trivial solution of the model. Using these solutions we show that the high density limit of the Friedberg-Lee type models depends on the leading power of the quark-σ coupling vertex. The numerical results are presented in Sec. 5

2 Soliton models with quark-meson coupling

Our starting point for studying the high density behavior of soliton matter is the Friedberg-Lee [6] non-topological soliton model, and we also consider related models like the chiral chromodielectric model of Fai, Perry and Wilets [7]. In their simplest versions, these models include only constituent quarks and a single scalar field σ that couples to the quarks. For the light quarks we shall assume $m_u = m_d = 0$. Extending these models in the spirit of the quark-meson coupling model, we introduce in addition two meson fields: namely, a scalar meson ϕ and a vector meson V_μ, which play important roles in quantum hadrodynamics. We assume these mesons couple linearly to the quarks. There is some freedom in the structure of the quark-meson vertex, in regard to its dependence on the soliton field σ. Using the Nielsen-Patkos Lagrangian [20], Banerjee and Tjon [21] have recently argued that in NTS models the quark-meson coupling should also depend on the scalar soliton field. Similar conclusions are reached by Krein, *et al.* [19]. However, we have found that this causes unwanted behavior within the mean field and Wigner-Seitz approximations used here (see Sec. 4), and so we report calculations that use σ-independent quark-meson couplings. As we shall see, this choice has the advantage of reproducing the Quantum Hadrodynamics equation of state at low densities.

Thus we take the Lagrangian density to have the form

$$\begin{aligned}\mathcal{L} &= \bar{\psi}\left[i\gamma^\mu\partial_\mu - m_f - (g(\sigma) + g_s\phi - g_v\gamma^\mu V_\mu)\right]\psi + \frac{1}{2}\partial_\mu\sigma\partial^\mu\sigma - U(\sigma) \\ &\quad + \frac{1}{2}\partial_\mu\phi\partial^\mu\phi - \frac{1}{2}m_s^2\phi^2 - \frac{1}{4}F_{\mu\nu}F^{\mu\nu} + \frac{1}{2}m_v^2 V_\mu V^\mu \qquad (1)\end{aligned}$$

where the σ field self interaction is assumed to be

$$U(\sigma) = \frac{a}{2!}\sigma^2 + \frac{b}{3!}\sigma^3 + \frac{c}{4!}\sigma^4 + B \ . \qquad (2)$$

The constants a, b and c are fixed so that $U(\sigma)$ has a local minimum at $\sigma = 0$ (inflection point if a=0) and a global minimum at $\sigma = \sigma_v$, the vacuum value. The mass of the glueball excitation associated with the σ field is given by $m_{GB} = \sqrt{U''(\sigma_v)}$.

The quark-σ coupling is taken to be

$$g(\sigma) = \begin{cases} g_\sigma \sigma & \text{for the FL model} \\ g_\sigma \sigma_v \left[\dfrac{1}{\kappa(\sigma)} - 1 \right] & \text{for the } \chi\text{CDM} \end{cases} \tag{3}$$

where the chromodielectric function $\kappa(\sigma)$ has the form

$$\kappa(\sigma) = 1 + \theta(x) x^{n_\kappa} [n_\kappa x - (n_\kappa + 1)] \ ; \ x = \sigma/\sigma_v \ , \tag{4}$$

In the following we will take $n_\kappa = 3$. In perturbative calculations that include gluons the dielectric function $\kappa(\sigma)$ is regularized in order to handle infinities in the one gluon exchange diagrams associated with a vanishing dielectric constant [7]. Such a regulation is also useful for our numerical work. Koepf et. al. [22] use the prescription

$$\kappa(\sigma) \longrightarrow \kappa(\sigma)(1 - \kappa_v) + \kappa_v \tag{5}$$

where κ_v is a constant often simply fixed at $\kappa_v = 0.1$. However, this regulation forces $g'(\sigma_v) = 0$, and we prefer instead to regulate as follows:

$$\kappa(\sigma) = 1 + \theta(x) x^{n_\kappa} [n_\kappa x - (n_\kappa + 1 - \kappa_v)]. \tag{6}$$

We find that properties of isolated solitons are independent of κ_v for values even as large as .1, but results become sensitive to κ_v at high densities. Here, we shall treat κ_v as an additional parameter.

The Euler-Lagrange equations corresponding to (1) are given by

$$[\gamma^\mu (i\partial_\mu + g_v V_\mu) - (m_f + g(\sigma) - g_s \phi)] \psi = 0 \tag{7}$$

$$\partial_\mu \partial^\mu \sigma + U'(\sigma) + g'(\sigma) \bar{\psi} \psi = 0 \tag{8}$$

$$\partial_\mu \partial^\mu \phi + m_s^2 \phi - g_s \bar{\psi} \psi = 0 \tag{9}$$

$$- \partial_\mu F^{\mu\nu} - m_v^2 V^\nu + g_v \bar{\psi} \gamma^\nu \psi = 0 \tag{10}$$

where $U'(\sigma) = \frac{dU(\sigma)}{d\sigma}$ and $g'(\sigma) = \frac{dg(\sigma)}{d\sigma}$. We solve Eqs. (7-10) in the mean field approximation: we replace the soliton field σ by a c-number $\sigma \longrightarrow \sigma(\vec{r})$ and the meson fields by their expectation values in the nuclear medium $\phi \longrightarrow <\phi>= \phi_0$ and $V_\mu \longrightarrow <V_\mu>= \delta_{\mu 0} V_0$, with ϕ_0 and V_0 constants. The approximation that the scalar and vector mesons fields can be regarded as constants while the soliton field is to depend on spatial coordinates stems from the long range nature of the light mesons and the short range nature of the soliton field due to the large glueball mass. In essence, the mesons are fast degrees of freedom and the glueball is slow, and we use a Born-Oppenheimer approximation. The resulting equations for the quark and the scalar soliton field are,

$$\left[-i\vec{\alpha} \cdot \vec{\nabla} + g_v V_0 + \beta (m_f + g(\sigma) - g_s \phi_0) \right] \psi_k = \epsilon_k \psi_k \tag{11}$$

$$- \nabla^2 \sigma + U'(\sigma) + g'(\sigma) \sum_{k(valance)} \bar{\psi}_k \psi_k = 0 \ . \tag{12}$$

We consider only valence quarks in our calculations.

3 The Wigner-Seitz approximation

In order to use Eqs. (11-12) for the study of high density nuclear matter, it is sufficient to concentrate on a unit cell and solve these equations with the appropriate boundary conditions. In this paper we shall assume that each unit cell contains a single nucleon, that is, our unit cell coincides with a Wigner-Seitz cell. The single nucleon energy E_N is a sum of two terms, the energy of the $n_q = 3$ quarks and the energy carried by the scalar soliton field σ:

$$E_N = n_q \epsilon_q + \int_{WS\ cell} d\vec{r} \left[\frac{1}{2} (\vec{\nabla}\sigma)^2 + U(\sigma) \right] . \tag{13}$$

The quark energy ϵ_q should be regarded as the eigenvalue of Eq. (11) for isolated bags, or as the average energy in the band for dense nuclear matter. It should be noted that E_N cannot be identified with the nucleon mass as it contains spurious center of mass motion [8]. In order to correct the center of mass motion in the Wigner-Seitz cell the nucleon mass at rest is taken to be

$$M_N = \sqrt{E_N^2 - < P_{cm}^2 >_{WS}} , \tag{14}$$

where $< P_{cm}^2 >_{WS} = n_q < p_q^2 >_{WS} + m_{GB} < (\vec{\nabla}\sigma)^2 >_{WS}$. The notation $<>_{WS}$ stands for an average over the Wigner-Seitz cell. Thus $< p_q^2 >_{WS}$ is the expectation value of the quark momentum squared and $m_{GB} < (\vec{\nabla}\sigma)^2 >_{WS}$ is the scalar soliton momentum squared. The latter average is obtained using a coherent state approximation [8], which is essentially a single mode correction to the classical soliton mass. We find this latter correction to be small with respect to the total mass of the soliton and ignore it henceforth (it is not clear how valid this single-mode approximation is: at higher density we find that this correction exceeds the energy of the σ field, with both going to zero).

At low density the band width vanishes and the quarks are confined in separate bags. Then we expect the following approximation to be most accurate: we assume the individual nucleons move around as a gas of fermions with effective mass M_N given by Eq. (14), and so we get the following estimate for the total energy density at nuclear density ρ_B:

$$\mathcal{E} = \frac{\gamma}{2\pi^2} \int_0^{k_F} dk k^2 \sqrt{M_N^2 + k^2} + \frac{1}{2} m_s^2 \phi_0^2 - \frac{1}{2} m_v^2 V_0^2, \tag{15}$$

where $\gamma = 4$ is the spin-isospin degeneracy of the nucleons. The Fermi momentum of the nucleons is related to the baryon density through the relation

$$\rho_B = \frac{\gamma}{6\pi^2} k_F^3 \ . \tag{16}$$

The total energy per baryon is given by $E_B = \mathcal{E}/\rho_B$. The constant scalar meson field ϕ_0 is determined by the thermodynamic demand of minimizing $\mathcal{E}$, which gives

$$\phi_0 = -\frac{\gamma}{4\pi^2 m_s^2} \int_0^{k_F} dk k^2 \frac{\frac{d}{d\phi_0}(E_N^2 - < P_{cm}^2 >)}{\sqrt{E_N^2 - < P_{cm}^2 >_{WS} + k^2}}. \tag{17}$$

The vector meson field is determined by averaging the Euler-Lagrange equation, Eq. (10), on a Wigner-Seitz cell yielding

$$V_0 = \frac{g_v}{m_v^2} < \psi^\dagger \psi >= \frac{g_v}{m_v^2} \sum_{k(valance)} < \psi_k^\dagger \psi_k >_{WS} \rho_B = \frac{n_q g_v}{m_v^2} \rho_B \; . \tag{18}$$

These equations are similar to those of quantum hadrodynamics, the difference here being that the nucleon now has structure and thus the meson fields couple to the nucleon through its quarks. At low density the nucleon mass approaches its free value, and our mean field equations reduce to those of quantum hadrodynamics.

The approximation used here for the nuclear system has often been adopted in modeling soliton matter, and is generally known as the Wigner-Seitz approximation. Each soliton is enclosed in a sphere of radius R such that $\frac{4\pi}{3}R^3 = 1/\rho_B$. On a periodic lattice the quark functions should satisfy Bloch's theorem $\psi(\vec{r}+\vec{a}) = e^{i\vec{k}\cdot\vec{a}}\psi(\vec{r})$ for the lattice vectors $\vec{a}$. Concentrating on a single cell the Bloch theorem gives boundary conditions for the quark spinors in that cell. Although one can solve these boundary condition in a self consistent manner [18], we shall make the simplifying assumption of identifying the bottom of the lowest band by the demand that the derivative of the upper component of the Dirac function disappears at R, and the top of that band by the demand that the value of the upper component is zero at R [17]. The quark spinor in the lowest band is assumed to be an s-state

$$\psi_k = \begin{pmatrix} u_k(r) \\ i\sigma \cdot \hat{r}\; v_k(r) \end{pmatrix} \chi, \tag{19}$$

and the resulting Euler-Lagrange equations for the spinor components are

$$\frac{du_k}{dr} + [m_f + g(\sigma) - g_s\phi_0 + (\epsilon_k + g_v V_0)]\, v_k = 0 \tag{20}$$

$$\frac{dv_k}{dr} + \frac{2v_k}{r} + [m_f + g(\sigma) - g_s\phi_0 - (\epsilon_k + g_v V_0)]\, u_k = 0 \; . \tag{21}$$

The corresponding equation, (12), for the soliton field assumes the form

$$-\nabla^2\sigma + U'(\sigma) + g'(\sigma)\rho_s(r) = 0. \tag{22}$$

The quark density ρ_q and the quark scalar density ρ_s are given by

$$\rho_q(r) = \frac{n_q}{4\pi\overline{k}^3/3} \int_0^{\overline{k}} d^3k \; \left[u_k^2(r) + v_k^2(r)\right] \; , \tag{23}$$

$$\rho_s(r) = \frac{n_q}{4\pi\overline{k}^3/3} \int_0^{\overline{k}} d^3k \; \left[u_k^2(r) - v_k^2(r)\right] \; , \tag{24}$$

where the band is filled up to $\overline{k}$. The quark functions are normalized so that there are three quarks in the Wigner-Seitz cell. The boundary conditions for the soliton field are $\sigma'(0) = \sigma'(R) = 0$. The boundary conditions for the quark functions at the origin are given by $u(0) = u_0$ and $v(0) = 0$, where u_0 is determined by the normalization condition

$$\int_0^R 4\pi r^2 dr (u(r)^2 + v(r)^2) = 1 \; . \tag{25}$$

The boundary conditions at $r = R$ are given by

$$u_b'(R) = 0 \ \Rightarrow \ v_b(R) = 0 \tag{26}$$

for the bottom of the lowest band, and

$$u_t(R) = 0 \tag{27}$$

for the top of the band. Using these equations we can solve for the corresponding ϵ_b and ϵ_t. We assume the tight-binding dispersion relation

$$\epsilon_k = \epsilon_b + (\epsilon_t - \epsilon_b)\sin^2\left(\frac{\pi k}{2k_t}\right), \tag{28}$$

and that the band is filled right to the top k_t. The assumption of such a dilute filling has been made previously[8], and we do not discuss it further. The quark functions corresponding to the energy ϵ_k can be simply obtained by integrating Eqs. (20) and (21) for each intermediate value ϵ_k. Substituting the dispersion relation into Eq. (13), the nucleon energy is given by

$$E_N = \frac{3n_q}{k_t^3}\int_0^{k_t} dk k^2 \epsilon_k + \int_0^R 4\pi r^2 dr\left[\frac{1}{2}\sigma'(r)^2 + U(\sigma)\right], \tag{29}$$

which is then used in (14) to determine the equation of state (15).

At higher density, where the bags begin to overlap, there is no reason to assume each quark is tightly bound to a single bag nor to impose that $3q$ groups move collectively with a well-defined momentum. Our equation of state cannot then be considered a good approximation at higher densities, and we must then find a different approximation for handling the kinetic energy. This is the subject of the next paper in this series. For now we are content with studying low density behavior, with a special interest in whether our approximations can still produce saturation at the expected density. In fact, as one approaches the empirical nuclear saturation density, the different models begin to distinguish themselves. This is discussed in detail in the next section.

4 The Trivial solution

The NTS models we are considering have a uniform plasma phase that is preferred at high densities. This corresponds to the solution $\sigma = 0$, so that the soliton bags "dissolve" and the quarks are free. For the original FL model, this solution is favored at unreasonably low densities. Moreover, in the WS calculations [8], for cell radii below ≈0.8-0.9 fm only a trivial constant solution can be found. For the more sophisticated analysis reported in [18], which includes higher partial waves in the quark wave functions and direct computation of the bands, the calculation breaks down already at a cell radius ≈1.4 fm. We view this as a fault of the model and not of the WS approximation, for regardless of whether our restricting the soliton to a single spherical cell represents a dense system well or not, our model of the nucleon should nevertheless allow the soliton to be squeezed to volumes well

below nuclear density before it breaks apart. (The saturation density of nuclear matter is ρ_0=0.17fm^{-3}, which corresponds to a WS cell radius R_0=1.12fm.) This leads us to look for improvements upon the original FL model, and the two particular extensions studied in this paper are generalizations of the quark-glueball coupling $g(\sigma)$ and the addition of explicit meson degrees of freedom. Before proceeding to the numerical results, let us look at how these extensions affect the trivial solution.

The trivial solution to the WS equations (20-22) is $u_k(r) = u_0$, $v_k(r) = 0$ and $\sigma(r) = \sigma_0$, where the constants u_0 and σ_0 are independent of both r and k. Strictly, for $k > 0$ this solution does not satisfy our boundary conditions; however, we find that below a given cell volume the numerical solution develops a singularity at the boundary in order to reproduce this preferred solution. Moreover, the more accurate self-consistent calculations of [18] for the FL model (which do not assume just s-wave states in the quark wave function) show that the width of the band also narrows sharply at the onset of the trivial solution, indicating that the k-dependence is not important. Thus in order to find the trivial solution that characterizes the breaking down of the WS calculation, we may assume that all the quarks are at the bottom of the band. This corresponds to squeezing an isolated soliton, and we insist that our model favors a nontrivial solution until the cell radius gets well below that corresponding to nuclear density.

In the present section we shall consider altering the quark-meson couplings in our models as suggested in Lagrangian [20, 21], namely:

$$g_s \rightarrow g_s g(\sigma), \qquad g_v \rightarrow g_v g(\sigma). \tag{30}$$

This will allow us to investigate whether the coupling to meson fields can help cure the breaking down of the FL model at too low density.

For the trivial solution, then, the normalization condition (25) gives

$$u_0 = \left(\frac{3}{4\pi R^3}\right)^{1/2} = \rho_B^{1/2}. \tag{31}$$

From Eq. (21) we find the quark eigenenergy is

$$\epsilon = m_f + g(\sigma_0)[1 - g_s\phi_0 + g_v V_0], \tag{32}$$

where σ_0 obeys Eq. (22), modified to account for the change in q-σ coupling, which leads to

$$U'(\sigma_0) = -3\rho_B g'(\sigma_0)[1 - g_s\phi_0 + g_v V_0]. \tag{33}$$

Solving for the mean field values of ϕ_0 and V_0, we have

$$\phi_0 = \frac{3g_s}{m_s^2}\rho_B g(\sigma_0) \qquad \text{and} \qquad V_0 = \frac{3g_v}{m_v^2}\rho_B g(\sigma_0), \tag{34}$$

yielding finally (for m_f=0)

$$\epsilon = g(\sigma_0)\left\{1 - 3\rho_B g(\sigma_0)\left[\frac{g_s^2}{m_s^2} - \frac{g_v^2}{m_v^2}\right]\right\} \tag{35}$$

and the total energy density

$$\mathcal{E} = 3\rho_B g(\sigma_0)\left\{1 - \frac{3}{2}\rho_B g(\sigma_0)\left[\frac{g_s^2}{m_s^2} - \frac{g_v^2}{m_v^2}\right]\right\} + U(\sigma_0). \tag{36}$$

This is clearly a spurious solution corresponding to putting all the quarks in the lowest level. One needs to add the kinetic energy correctly to get the true energy of the quark plasma.

We would like to select a model for which the trivial solution is found only at densities much higher than nuclear density, and we would like the quark mass ϵ to be zero in the preferred phase. This latter condition implies σ_0=0. However, for the FL model $g(\sigma) = g_\sigma \sigma$, and therefore σ_0=0 is not a solution of Eq. (33). Using Eqs. (34) and substituting for U', g' and g, for the FL model Eq. (33) becomes

$$a\sigma_0 + \frac{b}{2}\sigma_0^2 + \frac{c}{6}\sigma_0^3 = -3\rho_B g_\sigma \left[1 - 3\rho_B g_\sigma \left(\frac{g_s^2}{m_s^2} - \frac{g_v^2}{m_v^2}\right)\sigma_0\right]. \tag{37}$$

If we turn off the meson fields $g_s, g_v \to 0$, we see that the solution to (37) goes as $-\rho_B^{1/3}$ at large densities. Not only does this blow up as $\rho_B \to \infty$, but it gives the quarks an unphysical negative mass $\epsilon \sim -g_\sigma \rho_B^{1/3}$. On the other hand, if we turn on the meson fields and make the usual choice of parameters so that $g_s^2/m_s^2 > g_v^2/m_v^2$ (which is necessary for saturation), there is now a positive high density solution that goes as ρ_B^{-1}. However, there is still an unphysical negative solution, now diverging as ρ_B. Thus we do not expect the inclusion of the meson fields to cure the problem of the FL model.

Now let us consider a modified FL model in which we take the quark-glueball coupling to be $g(\sigma) = g_\sigma \sigma^2$. We shall call this the FL^2 model. Then instead of Eq. (37) we have

$$a\sigma_0 + \frac{b}{2}\sigma_0^2 + \frac{c}{6}\sigma_0^3 = -6\rho_B g_\sigma \sigma_0 \left[1 - 3\rho_B g_\sigma \left(\frac{g_s^2}{m_s^2} - \frac{g_v^2}{m_v^2}\right)\sigma_0^2\right]. \tag{38}$$

For this model the trivial solution $\sigma_0 = 0$ exists in the Wigner-Seitz approximation. There are also nonzero solutions, however. With the meson fields switched off there are two nontrivial solutions

$$\sigma_0 = -\frac{3b}{2c}\left\{1 \pm \sqrt{1 - \frac{8c}{3b^2}(a + 6\rho_B g_\sigma)}\right\}, \tag{39}$$

which exist only at densities $\rho_B < a(3b^2/8ac - 1)/6g_\sigma$. For the parameter choice used here, this corresponds to cell radii $R > 1.67$ fm. These solutions give the quarks a positive mass and do not necessarily signal any problems with the model. For nonzero q-σ coupling, the solutions exist also at high density, behaving as $\sigma_0 \propto \pm\rho_B^{-1/2}$. The quark effective mass (35) vanishes in this limit. Thus the FL^2 does not seem to have the problems of the FL model when using the WS approximation.

Finally, let us consider the χCD models. From Eqs. (3) and (4) we see that for small σ the coupling $g(\sigma)$ is of leading order n_κ in σ. This means that, regardless of whether the mesons are present, for the χCD model with $n_\kappa \geq 2$ there will be a solution to Eq. (33) such that $\sigma_0 = 0$. This corresponds to the desired free massless quark plasma phase, with

vanishing meson field averages, since then $g(0) = g'(0) = 0$. Furthermore, one can show that as $\rho_B \to \infty$ the only other solution has $\sigma_0 \sim \rho_B^{-1}$ and gives the quarks a positive mass that also vanishes in the high density limit. Thus we expect the χCD models to provide a more reasonable description of dense nuclear matter than does the FL model, for there is no unphysical trivial solution to the WS equations that will cause problems.

Indeed, the type of behavior predicted by our analysis of the trivial solution is reflected in our Wigner-Seitz calculations. As we show in Fig. 1, the χCD model exhibits Wigner-Seitz solutions down to very small cell radii (we never reached a breakdown point, taking R as low as 0.05fm), whereas the FL model breaks down at the expected point $R \approx 0.8$fm. The FL^2 model can be taken down to lower cell radii than the FL, breaking down at $R \approx .25$fm, well above the transition to the uniform plasma phase. However, the behavior of ϵ_b below $R = 1$fm for the FL^2 model does not seem desirable. This could be cured by allowing the quark-meson coupling to depend on σ, but we find then non-smooth transitions to new non-trivial solutions in all the NTS models discussed here. We find more reasonable results if we keep the quark-meson coupling independent of σ, and thus the χCD seems the preferable model. We shall present results only for this latter model in the next section.

5 Results

We have performed the calculations using a straightforward numerical integration of the equations of motion for the q and σ fields. The mean field ϕ_0 is found by directly minimizing the free energy (15). As a check, we have also performed some calculations with a relaxation routine, but this is far more time consuming. The numerical calculations with the χCD model were carried out using the following set of parameters

$$a = 50\,\mathrm{fm}^{-2}\ ,\ b = -1300\,\mathrm{fm}^{-1}\ ,\ c = 10^4,\ g_\sigma = 2,\ \kappa_v = 0.1\ . \tag{40}$$

The parameters of the potential $U(\sigma)$ are chosen to give a reasonable bag constant $B = 46.6\mathrm{MeV/fm}^3$ and glueball mass $m_{GB} = 1.82$GeV. The value of σ_v is calculated to be $.285\mathrm{fm}^{-1}$, the single soliton energy is 1391 MeV and the nucleon mass is 1176 MeV. The nucleon rms radius is 0.876 fm. The parameters were chosen to fit the rms radius and nuclear matter properties, resulting in a somewhat high value of the nucleon mass. We did not spend much effort in fine-tuning the parameters, however. As the short range repulsion provided by the vector field in QHD is provided by the Wigner-Seitz boundary conditions in the liquid soliton model, in what follows we shall take the coupling constant between the vector meson and the quarks to be zero, $g_v = 0$. On the other hand we shall treat g_s as a free parameter in order to study its effect on the soliton matter.

For completeness, we also list the parameter sets used for the other models studied in the previous section. For the FL model, we take the parameters as in Birse et. al. [17]. (This set was also used in Ref. [18].) The full set of parameters for the soliton model is,

$$a = 0.0\ , b = -700.43\,\mathrm{fm}^{-1}\ \ , c = 10^4\ , g_\sigma = 10.98\ . \tag{41}$$

These parameters correspond to a single soliton energy 1260 MeV, and nucleon mass 902 MeV after removing the center of mass motion. For the FL2 model we use the same potential parameters and a coupling $g_\sigma = 60\text{fm}^{-1}$.

We proceed to our presentation of the results for the χCD model. To our knowledge, this is the first application of this particular model to the study of dense matter. Previous work has dealt with few nucleon systems [8].

In Figs. 2 and 3 we show the fields $u(r)$ and $\sigma(r)$ for several values of the cell radius R. As can be seen from its behavior at the cell boundary, the quark field $u_k(r)$ displayed in Fig. 2 is that corresponding to the bottom of the band $k = 0$. Fig. 3 shows that the depth of the bag decreases only slighty as the cell radius is lowered, indicating that the quarks remain tightly bound. (Note that for the FL model, however, the bag depth actually increases with smaller R [17, 8].) That the quarks are tightly bound in the bag can be seen clearly in Fig. 4, where we display the quark density $\rho_q(r)$ given by Eq. (23). There is only a small overlap with quarks from neighboring cells even at radii below 1 fm. In Figs. 1-4, the quark-meson coupling has been set to zero.

In Fig. 5 the top and bottom of the lowest energy band is shown as a function of R for several values of the quark-meson coupling g_s. The point at which the band begins to form, $R \approx 1.6$fm, is not very sensitive to the value of g_s. On the other hand, the structure of the band depends strongly on the coupling to the scalar meson, becoming wider as g_s is increased. In Fig. 6 we present the energy of the soliton E_N given by Eq. (29), and in Fig. 7 we show the total energy per baryon E_B of the system, derived from Eq. (15). As expected, the introduction of the scalar meson to the the soliton matter results in attraction and saturation. The empirical nuclear saturation density corresponds to $R_0 = 1.12$ fm, whereas from Fig. 7 we see, for example, that our NTS nuclear matter energy per baryon has a minimum at $R \approx 1.35$fm for $g_s = 1$. The saturation energy is $E_B - M_N^{(as)} \sim 20$ MeV, as compared to the empirical value $E_{sat} = 16$ MeV. The compression modulus of nuclear matter is $K = R^2 d^2 E_B/dR^2$ at the equilibrium point: for the present model we find $K \approx 1170$MeV. This is to be compared to empirical estimates that usually lie in the range 100-500MeV, with $K = 200$MeV the generally accepted value[23]. These results should be regarded as only order of magnitude, as at higher density we are surely underestimating the kinetic energy of the system. We shall develop a more reasonable model of the liquid state, which leads to a more quantitatively accurate EOS for solitonic nuclear matter, in the next paper of this series.

The solution for the χCD model is stable down to very low values of R (at least as low as 0.05 fm), and it is apparent that with proper calibration this model can be used as an excellent starting point for the study of nuclear matter. Another important feature of this model is the increase of the nucleon rms with density, Fig. 8. This unexpected outcome of the model is in accord with the EMC effect. Checking the sensitivity of this effect to model parameters, we found that the increase in the rms is insensitive to recoil corrections, but might disappear with different choices of the soliton parameters.

6 Discussion

In this paper we have investigated a class of non-topological soliton models that generalize the Friedberg-Lee model. We have studied nuclear matter in the Wigner-Seitz approximation, where neighboring bags begin to overlap at higher density, as a means of distinguishing between the various models. The models differ in the precise form of the coupling between the quarks and the scalar gluon field, and in the presence and form of couplings to explicit meson fields. Of the models studied, we have found the chiral chromodielectric model to exhibit behavior best in line with phenomenological expectations. For this model, there is no breakdown in the Wigner-Seitz calculation as the cell radius is decreased, thus overcoming a serious shortcoming of the original FL model. We consider it a computational necessity to consider only constituent quarks and ignore colored gluons and sea quarks, and thus these restrictions along with the addition of explicit meson fields may be seen as an approximation to the original theory. The original χCD model is closely based upon QCD, exhibiting absolute confinement, and it is therefore satisfying to see that this model is selected by our studies of nuclear matter.

We include mesons along the lines of quantum hadrodynamics, and we use the mean field approximation. In our final calculations we have considered only the scalar meson, but it is straightforward to include also the vector meson, which should be done for fine-tuning the parameters. We note that we found it best to use a quark-meson coupling that is not modulated by the quark-glueball coupling, in contrast to that argued for in Refs. [19, 21]. Indeed, when using a $q-\phi$ coupling proportional to $g(\sigma)$, we find jumps to qualitatively different solutions as density is increased. The resulting curve of energy as a function of cell radius has several bumps, which is clearly an undesirable feature. However, this should not necessarily be taken as an argument against models that employ quark-meson couplings that depend on σ, but rather merely a statement that when using the mean field approximation it is more consistent to use a σ-independent q-ϕ coupling g_s. Indeed, one can view this coupling as a "mean field approximation" to a more fundamental coupling — namely, $g_s \sim \langle \tilde{g}_s g(\sigma) \rangle$.

In the end, then, we have used a χCD model with σ-independent coupling between quarks and the scalar meson. We find that the inclusion of the scalar meson provides a clear saturation point for nuclear matter and that a rough fit to both empirical nuclear matter and single nucleon properties can be obtained. One of the most interesting features found is an increase in the nucleon rms radius at intermediate densities, in line with the EMC effect. This is dependent on the presence of the scalar meson. There are clearly several refinements to our model and our calculations that must be considered before fine-tuning the parameters. Among these are the inclusion of other mesons in the model, the addition of perturbative gluonic effects, and an improved calculation of the quark wave function along the lines of Ref. [18]. One can also improve our handling of the spurious CM motion. Foremost, however, we need to improve our modeling of the liquid state.

In this paper we have used a low-density approximation in modeling nuclear matter with solitons. This consists in using a Wigner-Seitz approximation to calculate an effective nucleon mass. Then the kinetic energy is added to the system by taking the motion of the nucleons to be that of a Fermi gas. The assumptions of this picture include: the nuclear

medium restricts any given nuclear bag to a spherical cell; any given nucleon moves slowly, so that it can be constructed at rest and then boosted; the quarks remain tightly bound inside the bag; the nucleons move independently within the medium. Only the first of these assumptions can remain valid at high densities, where the nuclear medium will form a liquid in which each nucleon's motion is localized on short time scales and quarks need not remain tightly bound inside the bag. Since we are ultimately interested in studying the transition to a uniform quark plasma within our non-topological soliton model, we must do a better job of modeling the liquid state at high densities. This is the subject of our next paper.

Acknowledgments

We thank J.A. Tjon for helpful discussions.

References

[1] T. DeGrand, R.L. Jaffe, K. Johnson and T. Kiskis, Phys. Rev. **D12** (1975) 2060.

[2] T.H.R. Skyrme, Proc. Roy. Soc. **260** (1961) 127; Nucl. Phys. **31** (1962) 556.

[3] G.E. Brown, A.D. Jackson, M. Rho and V. Vento, Phys. Lett. **B154** (1984) 285; E. Wüst, L. Vepstas and A.D. Jackson, Phys. Lett. **B173** (1986) 217.

[4] S. Nadkarni, H.B. Nielsen and I. Zahed, Nucl. Phys. **B253** (1985) 308; S. Nadkarni and I. Zahed, Nucl. Phys. **B263** (1986) 23.

[5] T.S. Walhout, Nucl. Phys. **A484** (1988) 397; **A519** (1990) 816.

[6] R. Friedberg and T. D. Lee, *Phys. Rev.* **D15** (1977) 1694.

[7] G. Fai, R.J. Perry and L. Wilets, Phys. Lett. **B208** (1988) 1.

[8] L. Wilets, "Nontopological Solitons",World Scientific Lecture Notes in Physics Vol. 24, World Scientific (1989).

[9] J. D. Walecka, Ann. Phys. (N.Y.) **83** (1974) 491.

[10] B. D. Serot and J. D. Walecka, Advan. Nucl. Phys. vol. 16 (1986) 1.

[11] P. A. M. Guichon, Phys. Lett. **B200** (1988) 235.

[12] S. Fleck, W. Bentz, K. Shimizu and K. Yazaki, Nucl. Phys. **A510** (1990) 731.

[13] H. Müller and B. K. Jennings, nucl-th/9706049, (1997).

[14] P. A. M. Guichon, K. Saito and A. W. Thomas, Nucl. Phys. **A601** (1996) 349.

[15] P. G. Blunden and G. A. Miller, Phys. Rev. **C54** (1996) 359.

[16] X. Jin and B. K. Jennings, Phys. Rev. **C55** (1997) 1567.

[17] M. C. Birse, J. J. Rehr and L. Wilets, *Phys. Rev.* **C38** (1988) 359.

[18] U. Weber and J. McGovern, Phys. Rev. **C57** (1998) 3376; nucl-th/9710021, (1997).

[19] G. Krein, P. Tang, L. Wilets and A.G. Williams, Nucl. Phys. **A523** (1991) 548.

[20] H. B. Nielsen and A. Patkos, Nucl. Phys. **B195** (1982) 137.

[21] M. K. Banerjee and J. A. Tjon, Phys. Rev **C56** (1997) 497.

[22] W. Koepf, L. Wilets, S. Pepin and Fl. Stancu, Phys. Rev **C50** (1994) 614.

[23] E. Migli, T.L. Ainsworth and J. Speth, Phys. Lett. **B288** (1992) 1; E. Migli, Nucl. Phys. **A573** (1994) 395.

Figure 1: Energy of the bottom level of the band as a function of cell radius for the Friedberg-Lee (FL), modified Friedberg-Lee (FL^2) and Chiral Chromodielectric (χCDM) models

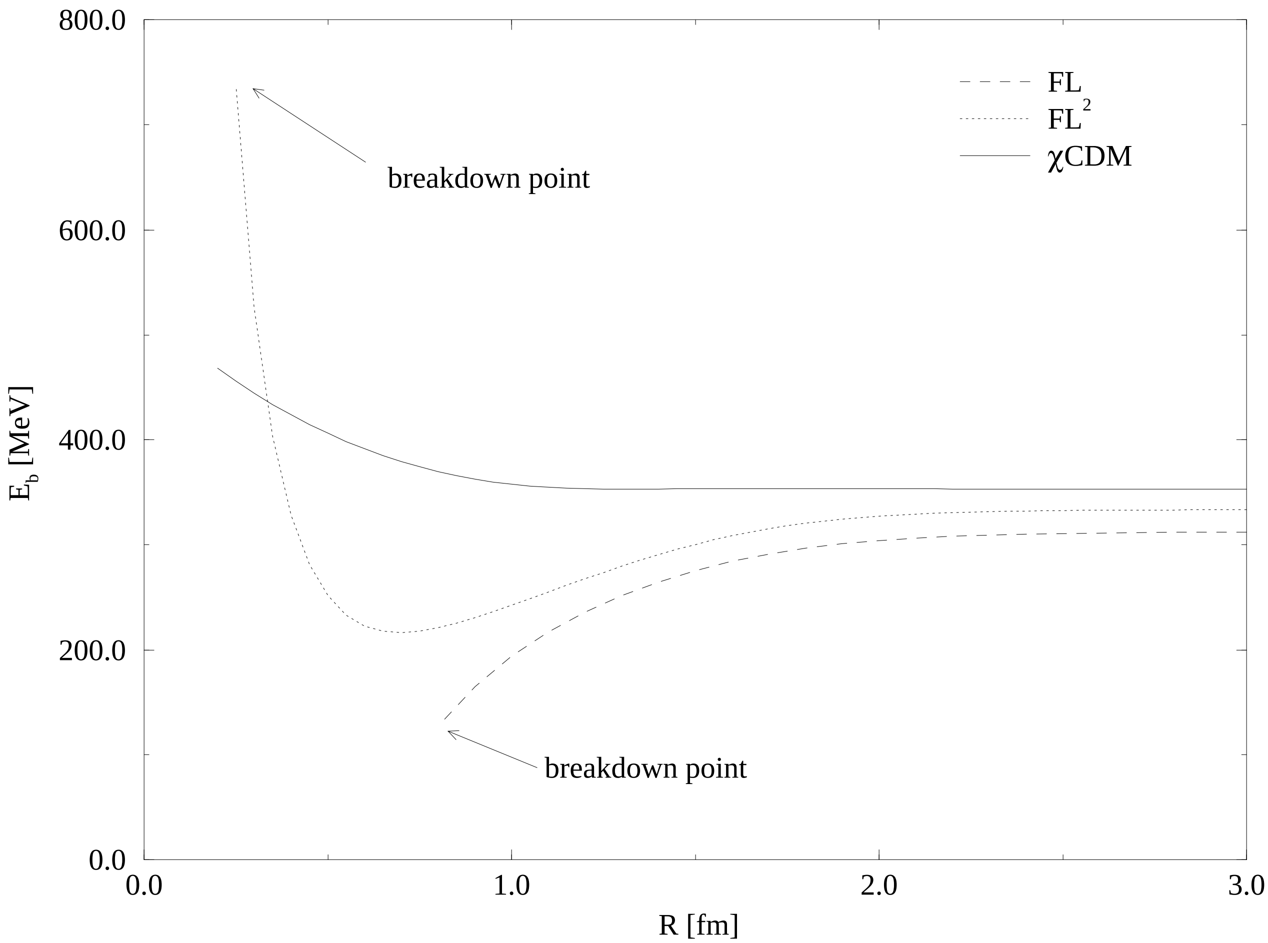

Figure 2: Upper component $u(r)$ of quark wave function at the bottom of the band for several cell radii R in χCD model

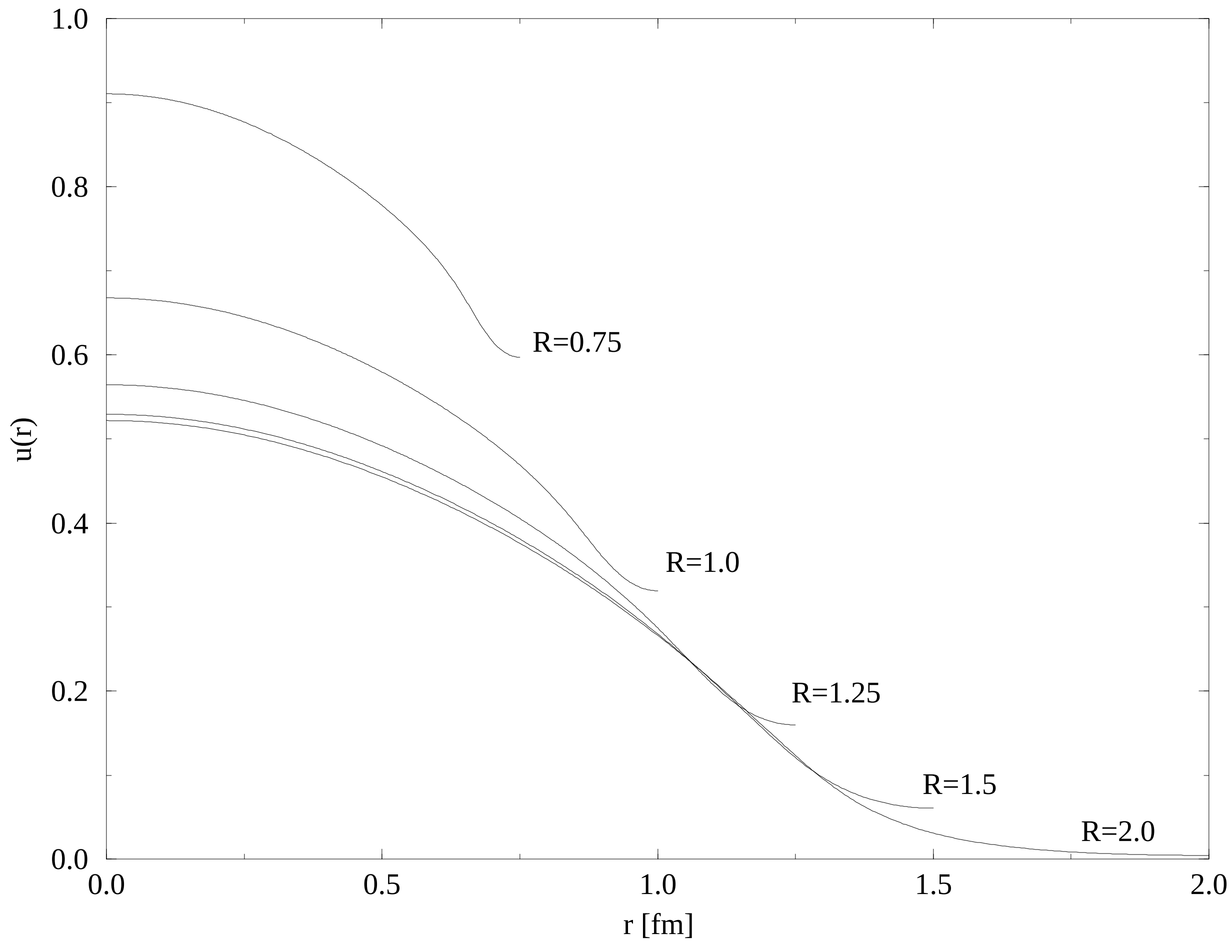

Figure 3: Soliton bag $\sigma(r)$ for several cell radii R in χCD model

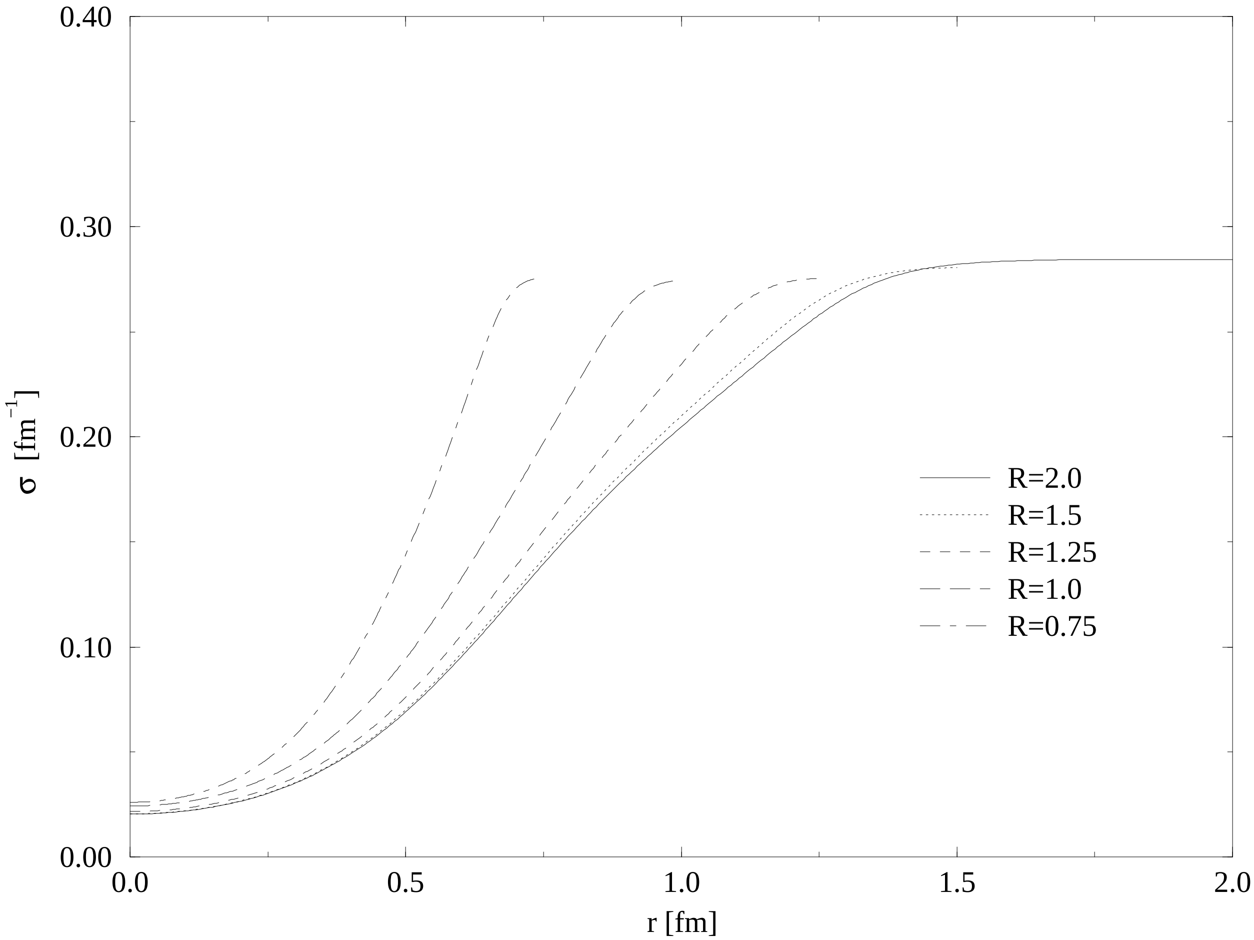

Figure 4: Quark density $\rho_q(r)$ for several values of R in χCD model

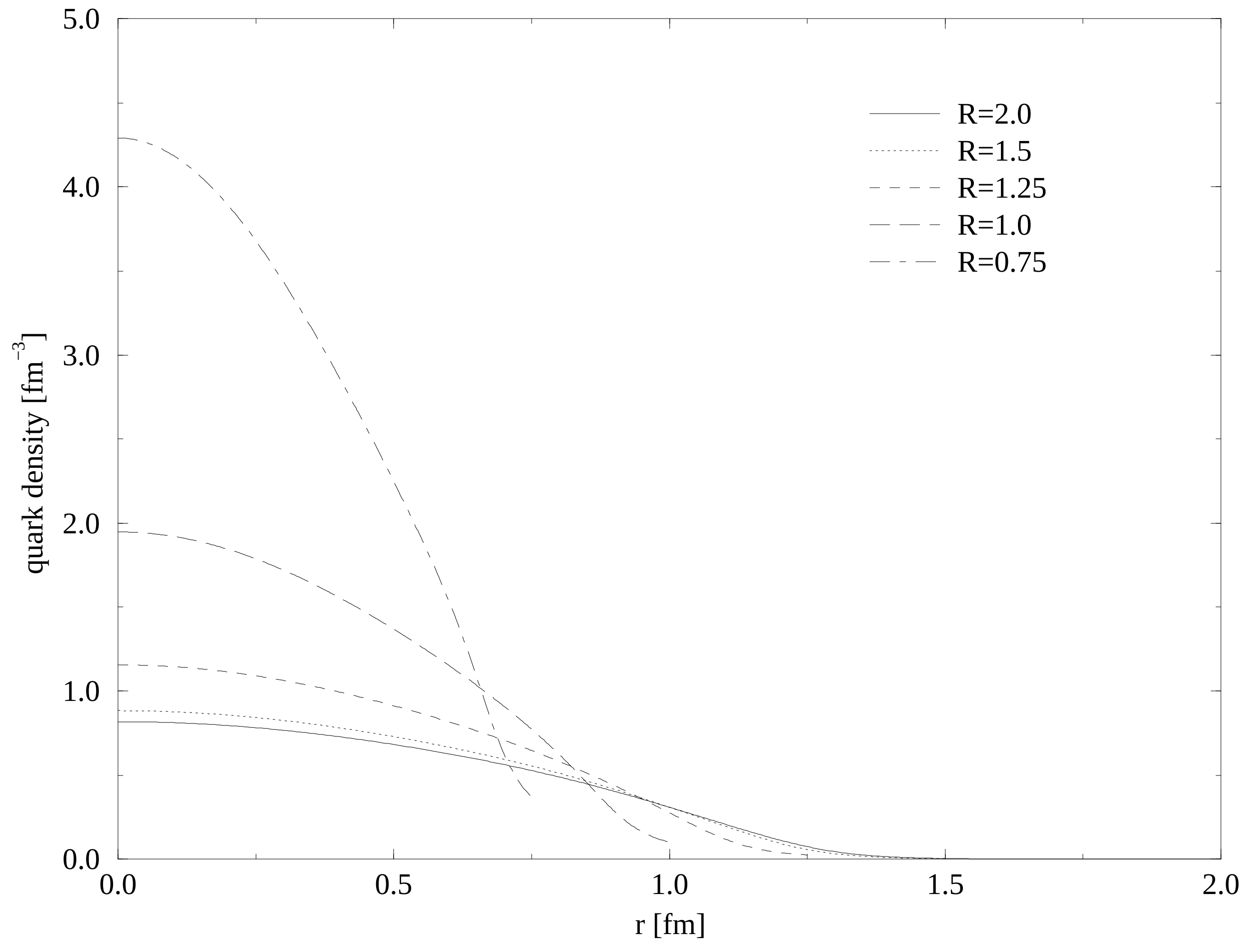

Figure 5: Energy of the bottom and top levels of the band versus R for several values of the quark-meson coupling g_s

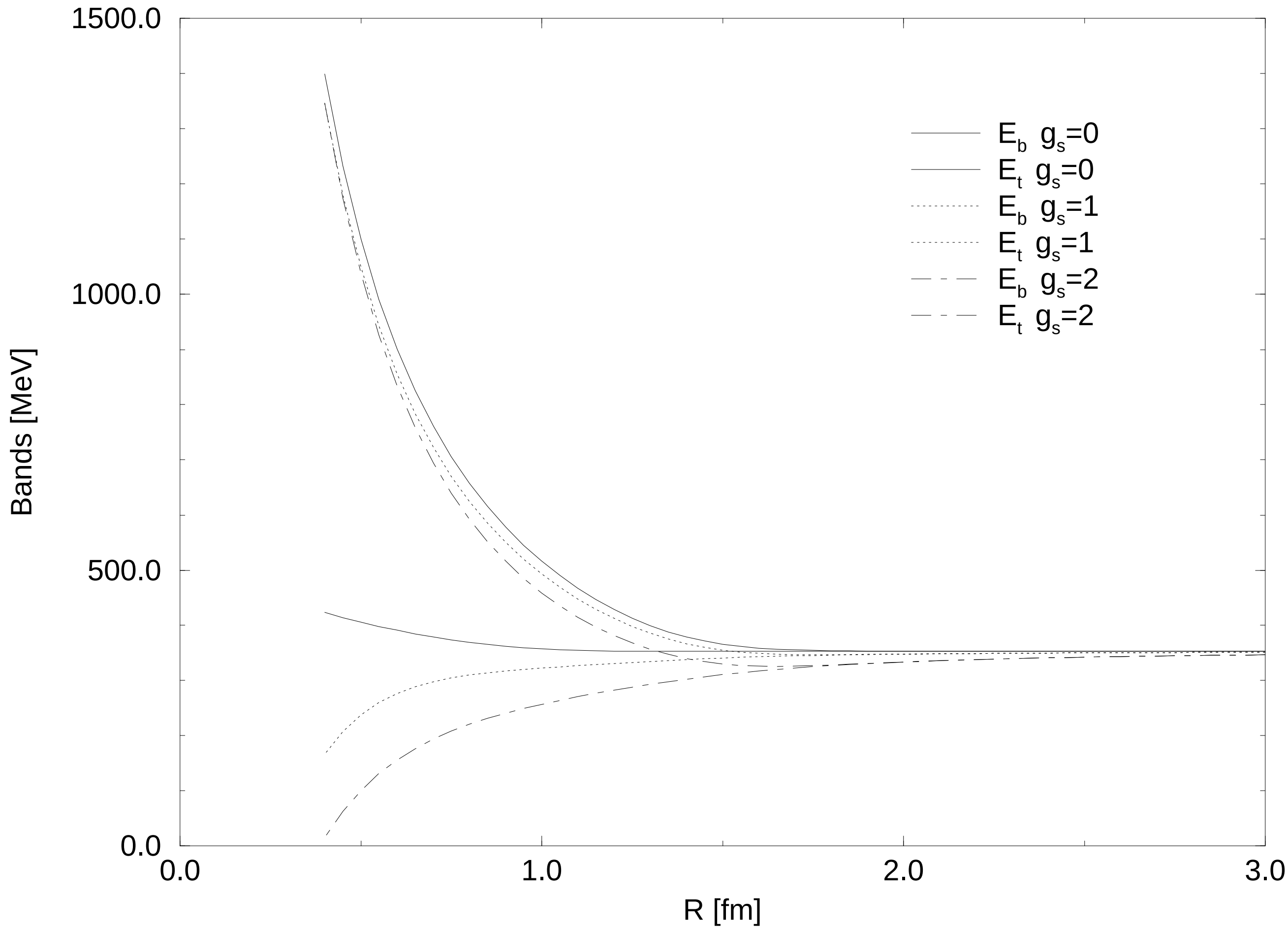

Figure 6: Soliton energy E_N (before subtracting spurious CM motion) for several values of g_s

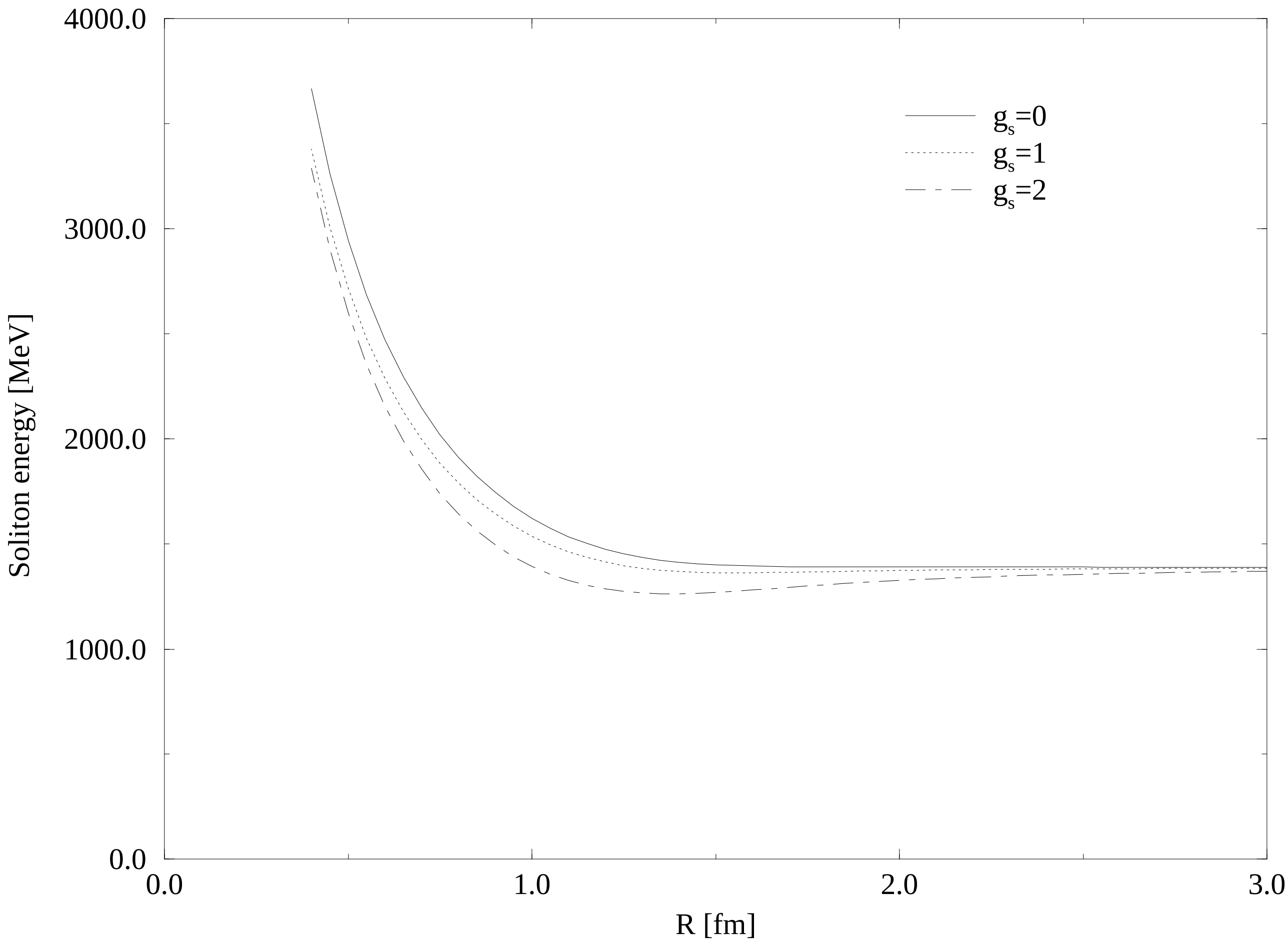

Figure 7: Energy per baryon E_B of nuclear matter as function of R and g_s in the χCD model

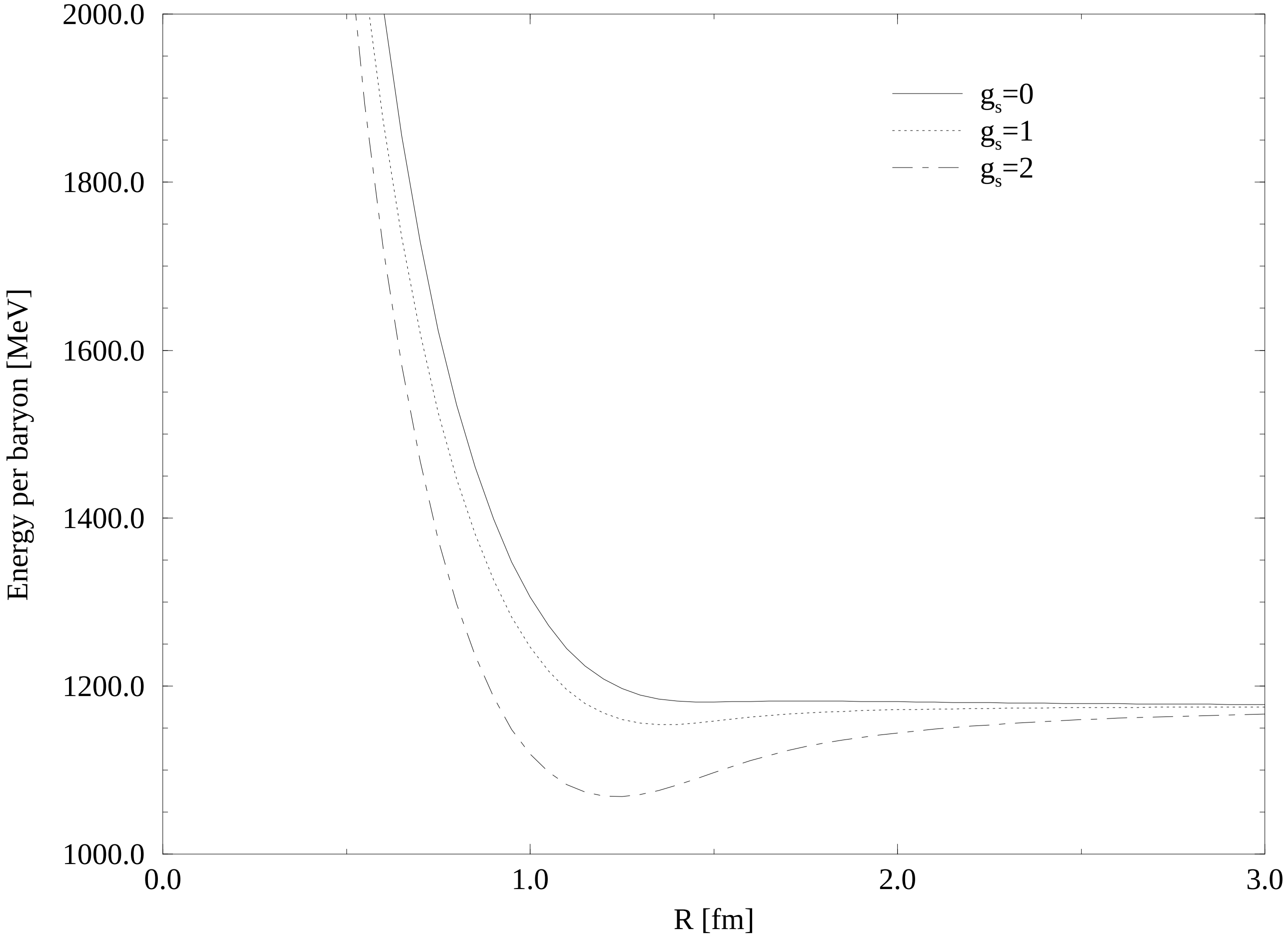

Figure 8: Nucleon rms radius as function of R and g_s in the χCD model